J. Phycol. **46,** 1252–1256 (2010)

DOI: 10.1111/j.1529-8817.2010.00916.x

ON THE ROLE OF THE CYTOSKELETON IN COCCOLITH MORPHOGENESIS: THE EFFECT OF CYTOSKELETON INHIBITORS[1]

Gerald Langer[2]

Institute of Environmental Science and Technology (ICTA), Universitat Autònoma de Barcelona (UAB), Bellaterra 08193, Spain

Lennart Jan de Nooijer

Department of Geochemistry, Faculty of Geosciences, Utrecht University, Budapestlaan 4, 3584 CD Utrecht, the Netherlands

and Kerstin Oetjen

Biogeosciences, Alfred Wegener Institute for Polar and Marine Research, 27570 Bremerhaven, Germany

The coccolithophore *Emiliania huxleyi* (Lohmann) W. W. Hay et H. Mohler was cultured in natural seawater with the addition of either the microtubule-inhibitor colchicine, the actin-inhibitor cytochalasin B, or the photosynthesis inhibitor 3-(3,4 dichlorophenyl)-1,1-dimethyl-urea (DCMU). Additionally, *E. huxleyi* was cultured at different light intensities and temperatures. Growth rate was monitored, and coccolith morphology analyzed. While every treatment affected growth rate, the percentage of malformed coccoliths increased with colchicine, cytochalasin B, and at higher than optimal temperature. These results represent the first experimental evidence for the role of microtubules and actin microfilaments in coccolith morphogenesis.

Key index words: **biomineralization; coccolith morphogenesis; coccolithophores; colchicine; cytochalasin B; cytoskeleton**

Abbreviations: **CAP, coccolith-associated polysaccharide; DCMU, 3-(3,4 dichlorophenyl)-1,1-dimethyl-urea**

Coccolithophores, unicellular haptophyte algae, surround themselves with a sphere of interlocking calcareous platelets, the coccoliths. A typical coccolith consists primarily of a radial array of complexly shaped interlocking crystals of calcite (Young and Henriksen 2003). The calcite unit cell has rhombohedral symmetry, and inorganically precipitated calcite crystals are typically rhombic. Although it is possible to identify rhombic crystal faces in coccoliths (Henriksen et al. 2004a), the overall form of a coccolith crystal is strongly modified (Young and Henriksen 2003). Obviously, coccolithophores rigorously control the morphology of the growing crystals. This control is also reflected in the diversity of coccolith morphology among coccolithophores. The morphogenesis of coccoliths is regarded as the ''most enigmatic part of biomineralization'' (Henriksen et al. 2004b, p. 726). The first step in the direction of deciphering this enigma was made more than a century ago when it was discovered that coccoliths are produced inside the coccolithophore cell and are subsequently extruded to become part of the coccosphere (i.e., the shell of a coccolithophore; Dixon 1900).

Since the advent of TEM in the middle of the 20th century, it has become feasible to study coccolithogenesis in greater detail. It was observed that the site of coccolith formation is a specialized Golgi-derived vesicle, the coccolith vesicle (Wilbur and Watabe 1963, Probert et al. 2007). Inside the coccolith vesicle, coccolith production occurs through two discrete processes, controlled nucleation of crystals and their subsequent growth (Young et al. 1999). By means of TEM, polysaccharides were detected inside the coccolith vesicle of *E. huxleyi*, located between the growing coccolith and the vesicle membrane (Van Der Wal et al. 1983). In contrast to *Pleurochrysis carterae* (Marsh et al. 2002), only one polysaccharide, the coccolith-associated polysaccharide (CAP), was isolated from *E. huxleyi* (Fichtinger-Schepman et al. 1981). It was shown that CAP can inhibit crystal growth (Borman et al. 1982) and influence crystal morphology by site-specific attachment to crystallographic steps (Henriksen et al. 2004a). Characterization and localization of CAP alone, however, cannot explain why growth of coccolith crystals proceeds in certain directions but not in others.

Another observation, crucial to understand coccolithogenesis, concerns the shape of the coccolith vesicle. In TEM sections, it was observed that the coccolith vesicle adopts the shape of the growing coccolith (Outka and Williams 1971, Klaveness 1972, Westbroek et al. 1984, Probert et al. 2007). This finding has led to the notion that the coccolith vesicle functions as a dynamic mould for the growing coccolith. A fibrillar structure adjacent to the coccolith vesicle was proposed to generate the force necessary for shaping the coccolith vesicle

[1]Received 30 December 2009. Accepted 20 July 2010.
[2]Author for correspondence: e-mail gerald.langer@awi.de.

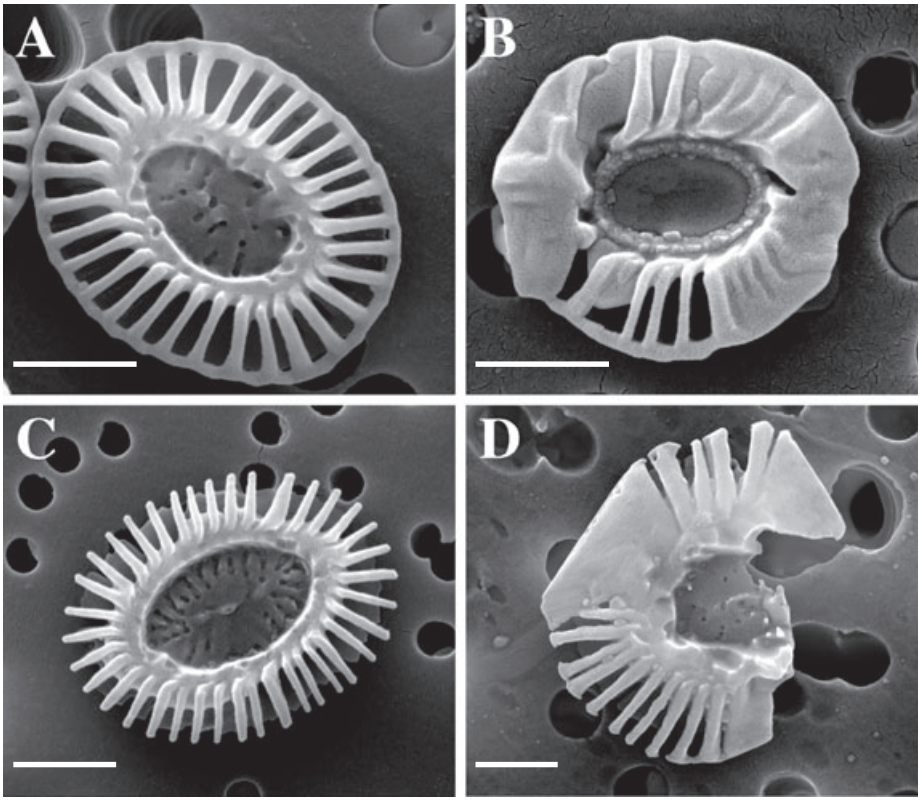

FIG. 1. SEM images of *Emiliania huxleyi* coccoliths. (A) Normal coccolith. (B) Malformed coccolith. (C) Incomplete coccolith, at ~80% growth. (D) Malformed and incomplete coccolith. Scale bars = 1 μm.

membrane (Klaveness 1972, 1976). It is now common to assume that the cytoskeleton comprises this fibrillar structure and is a crucial part of the machinery shaping the coccolith vesicle and therewith the coccolith (Westbroek et al. 1984, Didymus et al. 1994, Marsh 1994, 1999, Young et al. 1999, 2009, Marsh et al. 2002).

The cytoskeleton, discovered by Remak (1843) and Freud (1882), comprises three groups of filamentous proteins (i.e., intermediate filaments, actin microfilaments, and microtubules). Actin microfilaments and microtubules are essential for morphogenesis of diatom silica (Cohn et al. 1989).

The objective of the present study is to test whether actin microfilaments and microtubules are involved in coccolith morphogenesis. Therefore, we analyzed the coccolith morphology of *E. huxleyi* cells grown in natural seawater with the addition of either colchicine, a microtubule inhibitor (Eigsti 1938, Farrell and Wilson 1980), or cytochalasin B, an actin inhibitor (Maclean-Fletcher and Pollard 1980).

MATERIALS AND METHODS

Clonal cultures of *E. huxleyi* (strain RCC1238) were grown in aged, sterile-filtered (0.2 μm pore-size cellulose-acetate filters; Sartorius, Goettingen, Germany) North Sea seawater enriched with 100 μM nitrate, 6.25 μM phosphate, and trace metals and vitamins as in f/2 medium (Guillard 1975). Strain RCC1238 was obtained from the Roscoff Culture Collection (http://www.sb-roscoff.fr/Phyto/RCC). Cultures were grown under a 16:8 light:dark cycle. Experiments were carried out at a light intensity of 300 μmol photons $\cdot$ $m^{-2} \cdot s^{-1}$, with the exception of the experiments in which temperature (light intensity 400 μmol photons $\cdot$ $m^{-2} \cdot s^{-1}$) and light intensity were varied, in an adjustable incubator (Rubarth Apparate GmbH, Laatzen, Germany). Temperature for all experiments was 17°C, with the exception of the experiment in which temperature was varied. Cells were grown in dilute batch cultures, ensuring a quasi-constant seawater carbonate system over the course of the experiment (Langer et al. 2009). Each data point is the mean value of duplicate culture experiments, with the exception of the experiment with different cytochalasin B concentrations, in which only growth rate was determined. The latter experiment was done without replicates.

For determination of cell density, samples were taken at the beginning and the end of experiment and counted immediately after sampling using a Coulter Multisizer III (Beckman Coulter GmbH, Krefeld, Germany). Growth rate (μ) was calculated as follows:

$$\mu = (\ln c_1 - \ln c_0)\Delta t^{-1} \quad (1)$$

where c_0 and c_1 are the cell concentrations at the beginning and the end of experiment, respectively, and Δt is the duration of incubation in days.

Colchicine, cytochalasin B, DMSO, and DCMU were obtained from Sigma-Aldrich (Munich, Germany). Colchicine was dissolved in culture medium (concentration of stock solution was 25 mM). Cytochalasin B was dissolved in DMSO (concentration of stock solution was 50 mM). The highest cytochalasin B concentration used (100 μM) consequently entails 0.2% v/v DMSO. Finally, DCMU was also dissolved in DMSO (concentration of stock solution was 10 μM). The DCMU concentration used (0.01 μM) consequently entails 0.1% v/v DMSO. All stock solutions were freshly prepared prior to the start of the experiments.

Samples for SEM analysis were filtered on polycarbonate filters (0.8 μm pore-size), dried in a drying cabinet at 60°C for

24 h, then sputter-coated with gold-palladium using a Polaron Sputter Coater SC7600 (GaLa Gabler Labor Instrumente Handels GmbH, Bad Schwalbach, Germany). Imaging was performed with a Philips XL-30 digital scanning field-emission electron microscope (Philips GmbH, Hamburg, Germany). Four categories were used to describe the morphology of *E. huxleyi*: ''normal,'' ''malformed,'' ''incomplete,'' and ''incomplete and malformed'' coccoliths (Young 1994, for reference images for the categories, see Fig. 1). An average of ~350 coccoliths was analyzed per sample (Langer and Benner 2009).

RESULTS AND DISCUSSION

Colchicine caused a reduction in growth rate and hampered coccolith morphogenesis as a function of colchicine concentration. While the effect was negligible at 500 μM, it became visible at 750 μM and was strongest at 1,000 μM (Table 1). The latter colchicine concentration caused a marked shift of coccolith morphology toward malformed coccoliths, while the percentage of incomplete coccoliths remained similar.

Assuming that another cytoskeleton element (actin microfilaments) is also involved in coccolith morphogenesis, an initial experiment was conducted in which *E. huxleyi* was grown under different cytochalasin B concentrations, by monitoring growth rate only (Table 1). One of the adopted cytochalasin B concentrations (100 μM) had a considerable effect on growth rate and was therefore chosen for a subsequent experiment in which we determined both growth rate and coccolith morphology (Table 1). The effect of cytochalasin B on coccolith morphology was similar to that of colchicine (i.e., increasing the percentage of malformed coccoliths without a change in the percentage of incomplete coccoliths).

We conclude that the microtubule-inhibitor colchicine and the actin-inhibitor cytochalasin B disrupted microtubules and actin microfilaments, respectively, which were directly or indirectly involved in shaping the growing coccoliths. The fact that the percentage of incomplete coccoliths did not change (Table 1) may indicate that this malfunction in coccolithogenesis is not connected to microtubules and actin microfilaments. Also, the nucleation of the coccolith crystals does not seem to be impaired by colchicine and cytochalasin B, since the basic ring structure of the base of the tube (the locus of the proto-coccolith ring) appears to be largely unaffected

TABLE 1. Growth rates and percentages of normal versus malformed versus incomplete versus incomplete and malformed coccoliths.

			Morphology							
Sample	Growth rate (μ)	Standard deviation	Normal (%)	Standard deviation	Malformed (%)	Standard deviation	Incomplete (%)	Standard deviation	Incomplete and malformed (%)	Standard deviation
Colchicine III										
Control	1.35	0.01	91.90	0.17	3.27	1.02	1.93	0.47	2.90	0.71
500 μM	1.25	0.01	89.67	2.15	4.93	0.01	1.78	0.42	3.62	2.56
Colchicine IV										
Control	1.34	0.01	92.45	0.87	4.00	0.76	1.15	0.34	2.40	0.45
750 μM	0.95	0.00	81.27	1.66	8.93	2.85	2.47	1.03	7.33	0.16
Colchicine II										
Control	1.33	0.02	90.85	1.88	4.75	0.69	2.38	0.34	2.02	0.85
1,000 μM	0.59	0.04	42.25	4.10	22.09	1.54	2.53	0.14	33.14	2.69
Cytochalasin test										
0.1 μM	1.15	n/d	n/d	n/d	n/d	n/d	n/d	n/d	n/d	n/d
1 μM	1.18	n/d	n/d	n/d	n/d	n/d	n/d	n/d	n/d	n/d
10 μM	1.02	n/d	n/d	n/d	n/d	n/d	n/d	n/d	n/d	n/d
100 μM	0.20	n/d	n/d	n/d	n/d	n/d	n/d	n/d	n/d	n/d
Cytochalasin										
Control	1.51	0.03	86.99	3.96	6.33	3.38	2.42	1.50	4.25	2.08
100 μM	0.20	0.02	15.31	1.10	29.34	2.82	2.55	1.71	52.80	3.43
Photosynthesis										
Control	1.41	0.03	88.91	2.12	4.21	1.11	3.27	0.75	3.61	0.27
DCMU, 0.01 μM	0.58	0.01	92.82	1.55	3.49	0.08	3.07	1.35	0.62	0.13
Low light, 5–7 μmol photons $\cdot m^{-2} \cdot s^{-1}$	0.56	0.08	87.67	4.61	7.18	3.91	4.28	0.79	0.87	0.09
DMSO										
Control	1.23	0.15	n/d	n/d	n/d	n/d	n/d	n/d	n/d	n/d
0.04 vol %	1.41	0.01	n/d	n/d	n/d	n/d	n/d	n/d	n/d	n/d
0.1 vol %	1.44	0.03	n/d	n/d	n/d	n/d	n/d	n/d	n/d	n/d
0.2 vol %	1.41	0.02	n/d	n/d	n/d	n/d	n/d	n/d	n/d	n/d
0.5 vol %	1.41	0.00	n/d	n/d	n/d	n/d	n/d	n/d	n/d	n/d
Temperature										
10°C	n/d	n/d	80.99	10.77	7.99	1.77	1.86	0.44	9.16	8.56
15°C	n/d	n/d	86.87	0.27	3.39	0.53	3.43	1.19	6.31	0.39
20°C	n/d	n/d	89.08	1.23	4.05	0.87	3.17	0.37	3.69	0.01
25°C	n/d	n/d	28.86	1.33	24.67	2.58	1.73	1.27	44.74	2.52

DCMU, 3-(3,4 dichlorophenyl)-1,1-dimethyl-urea.

(Fig. 2). This observation complies with the notion of coccolith-crystal nucleation. It is generally accepted that nucleation of coccolith crystals is template mediated. This template is the rim of an organic scale located inside the coccolith vesicle, the so-called base plate (Westbroek et al. 1984). From this concept of crystal nucleation, it follows that a disruption of the cytoskeleton should not affect nucleation.

Since an effect on coccolith morphology always entails an effect on growth rate, it is not entirely inconceivable that the two cytoskeleton inhibitors affected merely microtubules and actin microfilaments involved in cell division (Schmit and Lambert 1988), and the reduced growth rate, in turn, hampered coccolith morphogenesis. If the latter was the case, every reduction in growth rate should increase the percentage of aberrant coccoliths. In order to test this hypothesis, we grew *E. huxleyi* under two different light intensities and four different temperatures and poisoned the cells with the photosynthesis-inhibitor DCMU (Wessels and Van Der Veen 1956). DCMU and low light caused a decrease in growth rate without affecting coccolith morphology (Table 1). This finding clearly shows that a decreased growth rate per se is not detrimental to coccolithogenesis, a conclusion supported by the data presented in Table 1 and in Langer et al. (2009).

Temperatures above the optimum for growth (~20°C, see Langer et al. 2009) disrupted coccolithogenesis, while temperatures below the optimum did not (Table 1). We would like to stress that percentages of aberrant coccoliths at 10°C do not differ from those at 15°C and 20°C; see the variability in the 10°C data (Table 1). Another *E. huxleyi* strain, however, displayed a decreased percentage of normal coccoliths under suboptimal temperatures (Watabe and Wilbur 1966), temperature ranges being comparable, hinting at strain-specific responses. Interpretation of temperature effects on coccolith morphology is not straightforward, since temperature affects physiologic processes on various levels (e.g., enzyme kinetics, structural integrity of proteins, membrane fluidity), and coccolithogenesis most likely involves processes on many of these levels. The observation that above-optimum temperature, but not below-optimum temperature, affects coccolithogenesis may be explained by disturbed membrane function due to increased membrane fluidity.

In comparison to the temperature effect, it is straightforward to explain the lack of effect of DCMU and low light (Table 1). Both DCMU and low light reduce photosynthetic rate, therewith diminishing the speed at which energy and reduction equivalents as well as organic carbon compounds for metabolism are provided. This trend should decrease coccolith production (which was indeed observed; see, e.g., Langer et al. 2007), but there is no reason to assume that it also disturbs the regulatory processes of coccolith morphogenesis.

Two of the poisons used in this study were dissolved in DMSO, namely, cytochalasin B and DCMU.

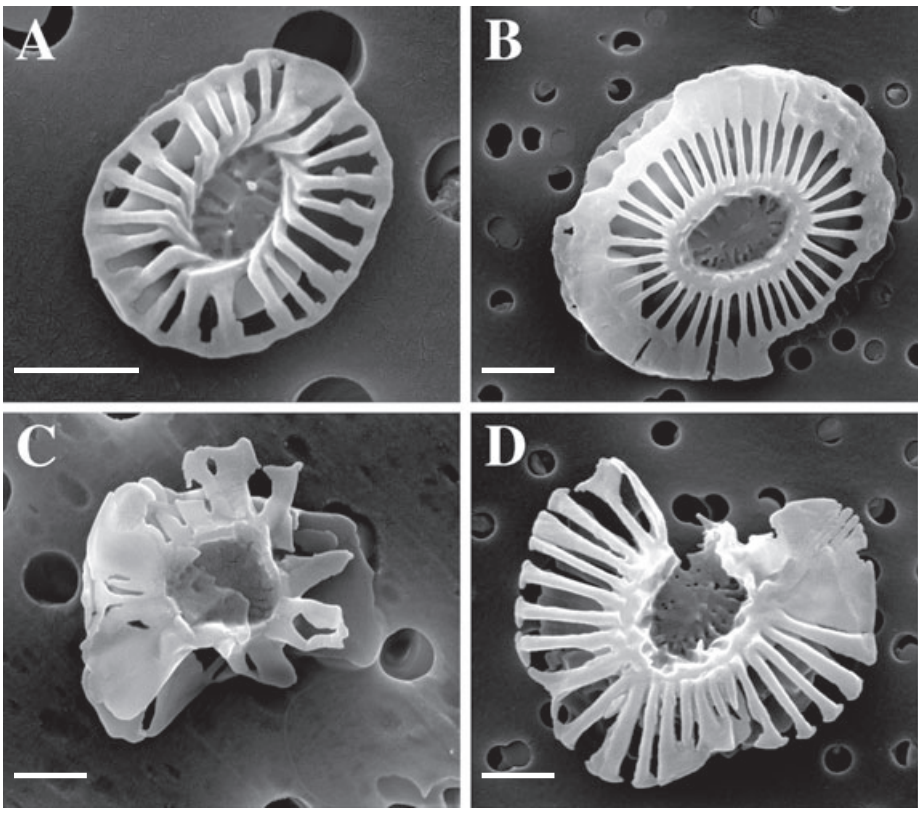

FIG. 2. SEM images of malformed *Emiliania huxleyi* coccoliths. Scale bars = 1 μm.

Being an organic solvent, DMSO can destroy membranes and therewith inflict considerable damage on cells. Therefore, we performed a separate experiment, in which we tested for the effect of DMSO. No change in growth rate was observed up to 0.5% v/v DMSO (Table 1). It can, therefore, be excluded that DMSO, and not cytochalasin B, caused the changes in growth rate and coccolith morphology (Table 1).

Taken together, the data presented here support the role of microtubules and actin microfilaments in coccolith morphogenesis. The precise mechanism of action of these two elements of the cytoskeleton remains to be discovered. It is certainly instructive that actin polymerization and microtubule polymerization have been shown to generate a pushing force against cell membranes causing cell protrusions (Condeelis 1993, Fygenson et al. 1997). The cytoskeleton may exert the necessary force for a mechanical control of coccolith-crystal growth.

We thank Friedel Hinz for SEM support. Thanks to Ian Probert, Jeremy Young, and Tina Brenneis for stimulating discussions and technical support. G. L. acknowledges financial support by the Spanish Ministry of Education (Juan de la Cierva program) cofunded by the European Social Fund and Ministry of Science and Innovation, and the program on Biologic Impacts of Ocean Acidification (BIOACID). L. J. de N. was sponsored through the European Project on Ocean Acidification (EPOCA) and the program on BIOACID.

Borman, A. H., De Jong, E. W., Huizinga, M., Kok, D. J., Westbroek, P. & Bosch, L. 1982. The role in $CaCO_3$ crystallization of an acid Ca^{2+}-binding polysaccharide associated with coccoliths of *Emiliania huxleyi*. *Eur. J. Biochem.* 129:179–83.

Cohn, S. A., Nash, J. & Pickett-Heaps, J. D. 1989. The effect of drugs on diatom valve morphogenesis. *Protoplasma* 149:130–43.

Condeelis, J. 1993. Life at the leading edge: the formation of cell protrusions. *Annu. Rev. Cell Biol.* 9:411–44.

Didymus, J. M., Young, J. R. & Mann, S. 1994. Construction and morphogenesis of the chiral ultrastructure of coccoliths from marine alga *Emiliania huxleyi*. *Proc. R. Soc. Lond. B Biol. Sci.* 258:237–45.

Dixon, H. H. 1900. On the structure of coccospheres and the origin of coccoliths. *Proc. R. Soc. Lond.* 66:305–15.

Eigsti, O. J. 1938. A cytologic study of colchicine effects in the induction of polyploidy in plants. *Proc. Natl. Acad. Sci. U. S. A.* 24:56–63.

Farrell, K. W. & Wilson, L. 1980. Proposed mechanism for colchicine poisoning of microtubules reassembled in vitro from *Strongylocentrotus purpuratus* sperm tail outer doublet tubulin. *Biochemistry* 19:3048–54.

Fichtinger-Schepman, A. M. J., Kamerling, J. P., Versluis, C. & Vligenhart, J. F. G. 1981. Structural studies of the methylated, acidic polysaccharide associated with coccoliths of *Emiliania huxleyi* (Lohmann) Kamptner. *Carbohydr. Res.* 93:105–23.

Freud, S. 1882. Über den Bau der Nervenfasern und Nervenzellen beim Flusskrebs. *Sitzungsber. Akad. Wien Math-Naturwiss. Classe* 85:9–46.

Fygenson, D. K., Marko, J. F. & Libchaber, A. 1997. Mechanics of microtubule-based membrane extension. *Phys. Rev. Lett.* 79:4497–500.

Guillard, R. R. L. 1975. Culture of phytoplankton for feeding marine invertebrates. *In* Smith, W. L. & Chanley, M. H. [Eds.] *Culture of Marine Invertebrate Animals.* Plenum Press, New York, pp. 29–60.

Henriksen, K., Stipp, S. L. S., Young, J. & Marsh, M. E. 2004a. Biologic control on calcite crystallization: AFM investigation of coccolith polysaccharide function. *Am. Mineralogist* 89:1586–96.

Henriksen, K., Young, J. R., Bown, P. R. & Stipp, S. L. S. 2004b. Coccolith biomineralisation studied with atomic force microscopy. *Palaeontology* 47:725–43.

Klaveness, D. 1972. *Coccolithus huxleyi* (Lohmann) Kamptner. I. Morphologic investigations on the vegetative cell and the process of coccolith formation. *Protistologica* 8:335–46.

Klaveness, D. 1976. *Emiliania huxleyi* (Lohmann) Hay and Mohler. III. Mineral deposition and the origin of the matrix during coccolith formation. *Protistologica* 12:217–24.

Langer, G. & Benner, I. 2009. Effect of elevated nitrate concentration on calcification in *Emiliania huxleyi*. *J. Nannoplankton Res.* 30:77–80.

Langer, G., Gussone, N., Nehrke, G., Riebesell, U., Eisenhauer, A. & Thoms, S. 2007. Calcium isotope fractionation during coccolith formation in *Emiliania huxleyi*: independence of growth and calcification rate. *Geochem. Geophys. Geosyst.* 8:Q05007, doi:10.1029/2006GC001422.

Langer, G., Nehrke, G., Probert, I., Ly, J. & Ziveri, P. 2009. Strain-specific responses of *Emiliania huxleyi* to changing seawater carbonate chemistry. *Biogeosciences* 6:2637–46.

Maclean-Fletcher, S. & Pollard, T. D. 1980. Mechanism of action of cytochalasin B on actin. *Cell* 20:329–41.

Marsh, M. E. 1994. Polyanion-mediated mineralization – assembly and reorganization of acidic polysaccharides in the Golgi system of a coccolithophorid alga during mineral deposition. *Protoplasma* 177:108–22.

Marsh, M. E. 1999. Coccolith-crystals of *Pleurochrysis carterae*: crystallographic faces, organization, and development. *Protoplasma* 207:54–66.

Marsh, M. E., Ridall, A. L., Azadi, O. & Duke, P. J. 2002. Galacturonomannan and Golgi-derived membrane linked to growth and shaping of biogenic calcite. *J. Struct. Biol.* 139:39–45.

Outka, D. E. & Williams, D. C. 1971. Sequential coccolith morphogenesis in *Hymenomonas carterae*. *J. Protozool.* 18:285–97.

Probert, I., Fresnel, J., Billard, C., Geisen, M. & Young, J. R. 2007. Light and electron microscope observations of *Algirosphaera robusta* (Prymnesiophyceae). *J. Phycol.* 43:319–32.

Remak, R. 1843. Ueber den Inhalt der Nervenprimitivröhren. *Arch. Anat. Physiol. Wiss. Med.* 1843:197–201.

Schmit, A.-C. & Lambert, A.-M. 1988. Plant actin filament and microtubule interactions during anaphase-telophase transition: effects of antagonist drugs. *Biol. Cell* 64:309–19.

Van Der Wal, P., De Jong, E. W., Westbroek, P., De Bruijn, W. C. & Mulder-Stapel, A. A. 1983. Ultrastructural polysaccharide localization in calcifying and naked cells of the coccolithophorid *Emiliania huxleyi*. *Protoplasma* 118:157–68.

Watabe, N. & Wilbur, K. M. 1966. Effects of temperature on growth, calcification, and coccolith form in *Coccolithus huxleyi* (Coccolithineae). *Limnol. Oceanogr.* 11:567–75.

Wessels, J. S. C. & Van Der Veen, R. 1956. The action of some derivatives of phenylurethan and of 3-phenyl-1,1-dimethylurea on the Hill reaction. *Biochim. Biophys. Acta* 19:548–9.

Westbroek, P., De Jong, E. W., Van Der Wal, P., Borman, A. H., De Vrind, J. P. M., Kok, D., De Bruijn, W. C. & Parker, S. B. 1984. Mechanism of calcification in the marine alga *Emiliania huxleyi*. *Philos. Trans. R. Soc. Lond. B* 304:435–44.

Wilbur, K. M. & Watabe, N. 1963. Experimental studies on calcification in molluscs and the alga *Coccolithus huxleyi*. *Ann. N. Y. Acad. Sci.* 109:82–112.

Young, J. R. 1994. Variation in *Emiliania huxleyi* coccolith morphology in samples from the Norwegian EHUX mesocosm experiment, 1992. *Sarsia* 79:417–25.

Young, J., Andruleit, H. & Probert, I. 2009. Coccolith function and morphogenesis: insights from appendage-bearing cocolithophores of the family Syracosphaeraceae (Haptophyta). *J. Phycol.* 45:213–26.

Young, J. R., Davis, S. A., Bown, P. R. & Mann, S. 1999. Coccolith ultrastructure and biomineralisation. *J. Struct. Biol.* 126:195–215.

Young, J. R. & Henriksen, K. 2003. Biomineralization within vesicles: the calcite of coccoliths. *In* Dove, P., De Yoreo, J. J. & Weiner, S. [Eds.] *Biomineralization. Reviews in Mineralogy and Geochemistry.* Mineralogic Society of America/Geochemical Society, Chantilly, Virginia, pp. 189–215.